LETTERS

Long-term stability of global erosion rates and weathering during late-Cenozoic cooling

Jane K. Willenbring[1] & Friedhelm von Blanckenburg[1]

Over geologic timescales, CO_2 is emitted from the Earth's interior and is removed from the atmosphere by silicate rock weathering and organic carbon burial. This balance is thought to have stabilized greenhouse conditions within a range that ensured habitable conditions[1]. Changes in this balance have been attributed to changes in topographic relief, where varying rates of continental rock weathering and erosion[1,2] are superimposed on fluctuations in organic carbon burial[3]. Geological strata provide an indirect yet imperfectly preserved record of this change through changing rates of sedimentation[1,2,4]. Widespread observations of a recent (0–5-Myr) fourfold increase in global sedimentation rates require a global mechanism to explain them[4–6]. Accelerated uplift and global cooling have been given as possible causes[2,4,6,7], but because of the links between rates of erosion and the correlated rate of weathering[8,9], an increase in the drawdown of CO_2 that is predicted to follow may be the cause of global climate change instead[2]. However, globally, rates of uplift cannot increase everywhere in the way that apparent sedimentation rates do[4,10]. Moreover, proxy records of past atmospheric CO_2 provide no evidence for this large reduction in recent CO_2 concentrations[11,12]. Here we question whether this increase in global weathering and erosion actually occurred and whether the apparent increase in the sedimentation rate is due to observational biases in the sedimentary record[13]. As evidence, we recast the ocean dissolved $^{10}Be/^{9}Be$ isotope system as a weathering proxy spanning the past ~12 Myr (ref. 14). This proxy indicates stable weathering fluxes during the late-Cenozoic era. The sum of these observations shows neither clear evidence for increased erosion nor clear evidence for a pulse in weathered material to the ocean. We conclude that processes different from an increase in denudation caused Cenozoic global cooling, and that global cooling had no profound effect on spatially and temporally averaged weathering rates.

Studies of both the suspended and the dissolved loads of the world's largest rivers and of hill-slope denudation have shown a strong link between physical erosion and chemical weathering[8,9]. Even though the exact mechanisms linking physical erosion rates with chemical weathering fluxes are still unknown, there is general agreement that high rates of physical erosion supply fresh mineral surfaces to the weathering environment[9]. Steep mountain slopes such as those in areas of active uplift often have the highest rates of total denudation. Thus, tectonically active areas should be coupled with large silicate weathering fluxes[2,4], and the atmospheric CO_2 withdrawn in this way should then be disposed of in the oceans' carbonate sediments[1]. Similarly, in basins surrounding active mountain belts, a substantial fraction of atmospheric CO_2 is sequestered through the terrestrial biosphere in the form of buried particulate organic carbon[3]. The consequences of the suggested fourfold global increase in Pliocene–Quaternary sedimentation rates[5,6] and, by inference, erosion rates should be associated with a similar increase in silicate weathering, carbonate sedimentation, organic carbon burial and, consequently, increased CO_2 drawdown (Fig. 1).

Atmospheric CO_2 concentrations derived from ocean palaeo-pH and stomatal indices do not testify to a significant decrease over this period. Concentrations were around 300 parts per million by volume (p.p.m.v.) during the Pliocene and Miocene epochs[11]. The significant drop from ~1,000 p.p.m.v. occurred long before the apparent increase in erosion. In particular, during the Pliocene and the Quaternary period, the fourfold increase in erosion was accompanied by only a minor drop in atmospheric CO_2 (refs 11, 12; Fig. 1). One proposed source of abated CO_2 drawdown during the past 12 Myr is a feedback caused by land plants that accelerated chemical weathering, attenuated long-term CO_2 concentration changes and prevented a transition into ice-house conditions during this apparent increase in erosion[15]. Another hypothesis is that chemical weathering and physical erosion are not linked in as straightforward a way as previously

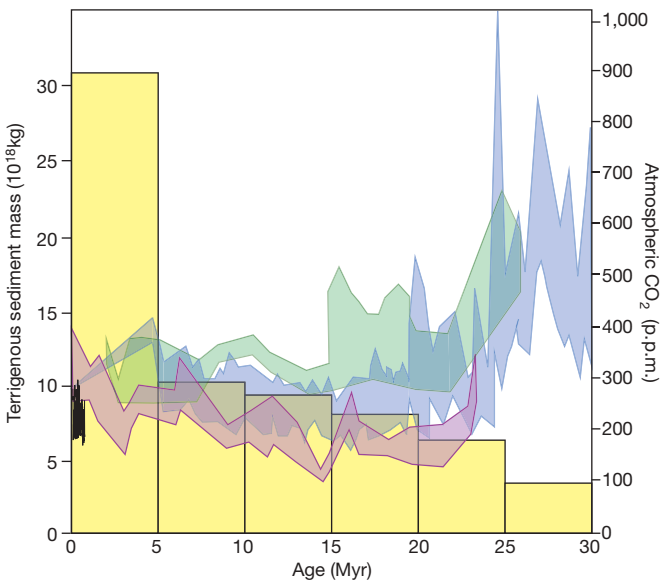

Figure 1 | Terrigenous sediment input into the oceans through the late-Cenozoic era and atmospheric CO_2. Yellow bars show global terrigenous sediment accumulation in oceans[5]. Values are separated into bins with an interval of 5 Myr and appear to increase abruptly during the past 5 Myr. The CO_2 data compilation is derived from a number of independent proxies and shows steady atmospheric concentrations from the mid-Miocene epoch to today (pre-industrial values) despite the observed increase in terrigenous sediment accumulation. Records include the stable boron isotopes in planktonic foraminifera (purple band), the stomatal distribution in the leaves of C_3 plants (green band), the stable carbon isotopes in alkenones (blue band) and air trapped in ice cores from Antarctica (thin black line). Each colour band spans the associated data points and their uncertainties. See Supplementary Information for additional details, uncertainties and references.

[1]Deutsches GeoForschungsZentrum GFZ, Section 3.4: Earth Surface Geochemistry, Telegrafenberg, D-14473 Potsdam, Germany.

thought. For example, in quickly eroding Himalayan-style environments, frequent, high-magnitude mass-wasting events decrease the soil cover and potentially cause lowered rates of silicate weathering[16]. Yet this plug of unweathered detritus and terrestrial carbon could still contribute to global CO_2 drawdown, depending on the contribution of silicate mineral dissolution to CO_2 drawdown that may take place in the basins within and surrounding mountain belts.

Variations in the silicate weathering flux have so far been difficult to quantify using sedimentary and isotope proxies[2]. The additional CO_2 flux from the burial of recent organic matter in the depositional basins surrounding active mountain belts, however, has been quantified using the stable isotopes of carbon measured in marine carbonates deposited over time[3]. Even though these reconstructions do not detect the absolute rates of organic carbon erosion and burial, an increase in the supply and burial of non-fossil carbon from young biomass that might have accompanied the apparent late-Cenozoic fourfold increase in erosion in basins experiencing high rates of terrigenous erosion and sedimentation[17] would show up as a similar increase in the size of the reservoir. However, at least for the past few million years, such an increase in the burial of young biomass is not apparent[3].

The impetus for the suggested global link between erosion and Quaternary global climate change described above stems from widespread observations that the mass of sediment and rock accumulated in oceans in the past 5 Myr is substantially larger than that accumulated in any previous interval[4–7] (Fig. 1). However, we suggest here that this synchronous increase may be an artefact introduced by observation and measurement biases. First, sedimentation rates today are usually measured where deposition is ongoing and rates are currently high. Second, the timescale over which rates are measured has a profound effect on measured rates[10,13]. Observations of real changes in accumulation rate through geologic time, such as the postulated fourfold rate increase over the past 5 Myr, require that, once deposited, sediment is completely preserved through geological time. Even after correcting for compaction of the lower sections of sedimentary cores, this is rarely the case because of the resulting decreased probability of preservation with age[10,13,18]. Hence, apparent deposition rates depend on the timescale of the measurement. Third, owing to the vagaries of chronological control through geological time, the timescale over which accumulation is measured is positively related to the age of the strata[18]. As such, rates are rarely measured over a constant time interval throughout a stratigraphic section and tend to decrease with geological age[13]. Fourth, given sufficient time, even depositional basins may be inverted and the reverse process (erosion of sediment) observed, leading to progressively decreasing strata volumes.

Figure 2 investigates this relationship for large temporal and spatial scales such as ocean deposits[5] (Fig. 2a), sedimentary deposits surrounding the Alps[19] (Fig. 2b), India[20] (Fig. 2c) and global recent-to-Cambrian rock volumes[21] (Fig. 2d). The decrease in deposition rate with geological time is apparent and follows the power law

$$\text{rate} = \text{constant} \times \text{time}^{\gamma - 1} \quad (1)$$

which has a slope of $\gamma - 1$ in logarithmic coordinates[13]. In all these cases (Fig. 2), the power coefficient is -0.5 ($\gamma = 0.5$); together they

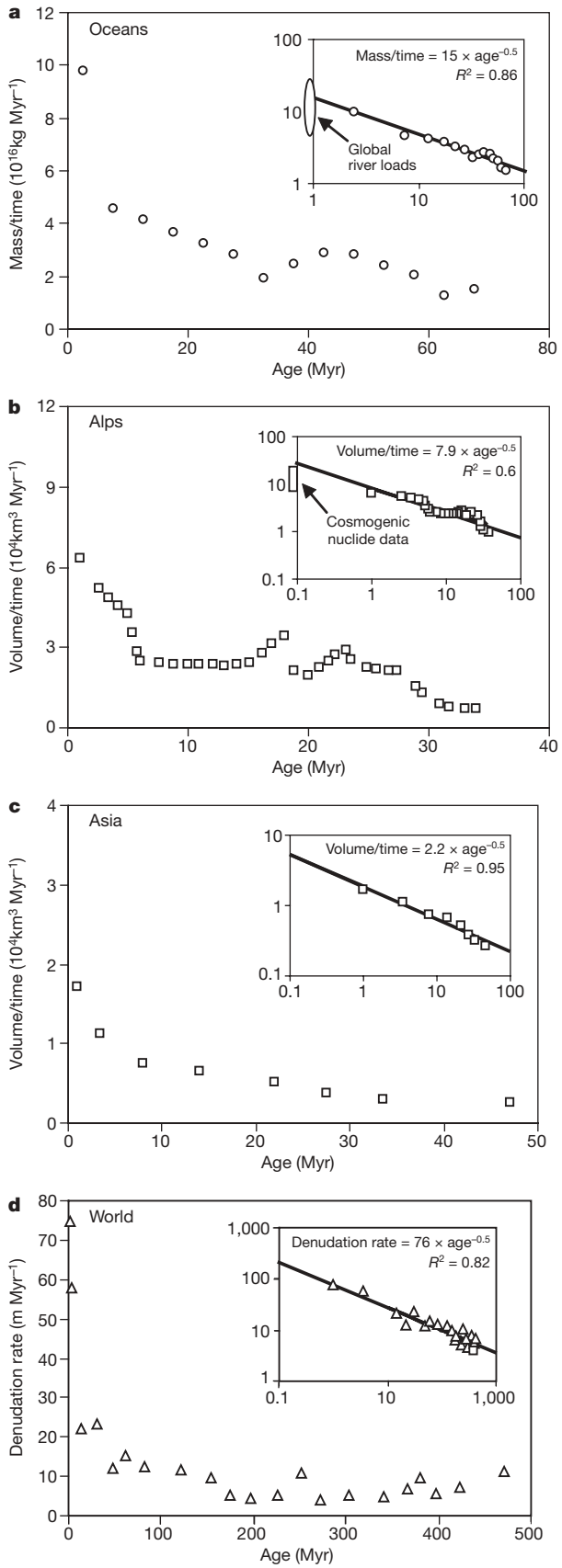

Figure 2 | Sediment accumulation rates and erosion rates as functions of geological time. Four representative environments in which erosion and sedimentation rates change with time. Values are plotted at age midpoints. Insets, same data plotted on a log–log scale. **a**, Global values for ocean basin sediment accumulation[5]. The ellipse in the inset shows the modern riverine flux range[22], which matches that expected for the flux plotted on a $\sim 10^5$–10^6-yr timescale. **b**, Volumetric erosion rates for the past 10 Myr from the European (Eastern and Western) Alps[19]. Rates were estimated from measurements of sediment accumulation in basins around the Alps and were corrected for compaction. In the inset, average cosmogenic isotope measurements[23] provide an estimate for recent millennial-scale denudation rates. **c**, Mass accumulation rates from 18 mostly offshore sedimentary basins in Asia after the initial India–Asia collision[20]. **d**, Global Pliocene-to-Cambrian land and ocean accumulations (by volume)[21] and Quaternary ocean accumulation[5]. All rock volumes were translated to denudation rate by normalizing for the area of continents that were exposed above sea level at that time[22]. All four environments share a common exponent of -0.5 (equation (1)), which is consistent with processes of stochastic deposition and erosion within the sedimentary deposits[10,13].

show similar scaling that spans four orders of magnitude and that is consistent with random net deposition, hiatus and erosion of sediment such that the net accumulation rate is the sum of all surface change divided by its age[13]. An exponential decrease in rates with time would explain much—but not all—of the observed recent (0–5-Myr) increase in terrigenous ocean sediment[5–7]. An exponential decrease, however, only takes into account fractional destruction of exposed rock area with time[18]; stochastic sediment transport and decreased preservation with age is described best by a power law (equation (1))[13].

In the logarithmic presentation (Fig. 2), the interception with the y axis provides an erosion rate on a timescale that is so close to modern times that recently measured rates potentially offer an independent benchmark with which this interpolated rate can be compared. Recent advances in our ability to determine modern and late-Holocene rates of erosion provide a wealth of such erosion rates. Indeed, these curves appear to intersect modern erosion rates of 40–70 m Myr^{-1} obtained from river load data[22] (Fig. 2a). In the Alps, where a large number of rates have been measured from basin accumulation[19], cosmogenic isotopes and lake infills[23], remarkable agreement exists between time-averaged and more recent rates (Fig. 2b), given this power-law relationship. The implication of this agreement is that even if these mountains are eroding at a rapid modern pace, they may have been doing so for the past 10–20 Myr.

A common assumption remains, namely that Quaternary glaciation increased the global delivery of sediment[4,7]. However, even in settings where glaciers can efficiently erode and transport material, a growing body of work demonstrates that only parts of the margins of such continents or orogens made of weak, friable bedrock formerly covered with ice were eroded significantly during glaciations[24,25]. The interiors of Northern Hemispheric ice sheets, analogous to the modern East Antarctic ice sheet, were often frozen to the underlying substrate and acted as a protective cover during the majority of the glacial intervals even near the southern margin of the Laurentide ice sheet[24,25]. In those cases in which ice did produce thick piles of glacial debris, these glacial deposits were often recycled from previous glaciations[26] and contributed little to the net delivery of sediment to the oceans.

The hypothesis of a lack of a recent increase in the global erosion rate and the inferred suggestion of steady silicate weathering rates requires an independent test not compromised by timescale issues. Geochemical proxies for global weathering rates potentially provide such a test[2]. However, radiogenic isotopes (Sr, Nd, Hf, Os and Pb) as measured in ocean sediment time series are proxies for many processes related to denudation style and source-rock isotope composition but are not necessarily good indicators of the weathering flux magnitude[2,26]. We suggest here that ocean records of the ratio of the sea water's dissolved stable isotope ^{9}Be, derived from continental denudation, to the sea water's dissolved constant-flux meteoric isotope ^{10}Be (ref. 27) show no increase in weathering flux over the past 12 Myr. This decay-corrected ^{10}Be/^{9}Be ratio remained constant over the past 12 Myr when measured in chemical ocean deposits such as Fe–Mn crusts precipitated from sea water or the authigenic phase of deep-sea sediments[14] (Fig. 3). Both faithfully record the sea water's dissolved ^{10}Be/^{9}Be ratio at the time of precipitation.

Most of the flux of cosmogenic ^{10}Be to the ocean has a direct atmospheric origin. Although variations in geomagnetic field strength and changes in solar modulation produce fluctuations in its flux, these are averaged out over the sampling intervals in the data sets[14,28] such that the flux over the oceans is roughly constant at 1×10^{6} atoms cm^{-2} yr^{-1}. Fluvial erosion also adds ^{10}Be to the oceans, but this flux is also roughly constant at steady state between production and removal by either erosion or radioactive decay, regardless of the denudation rate[27]. Hence, continental erosion is unlikely to introduce long-term variations in the ocean's ^{10}Be budget.

In contrast, ^{9}Be in the ocean has a terrestrial origin, with most derived from fluvial inputs to the oceans[27–29] and an insignificant portion from dust (see Supplementary Information for the full quantification of this mass balance). Initially, ^{9}Be accumulates in soils from partial dissolution of silicate minerals that host ~2 p.p.m. ^{9}Be and either binds to particles or remains in the dissolved form. The total amount of ^{9}Be that is either adsorbed to suspended particles in rivers or is transported in the dissolved form is directly dependent on the weathering extent of the source rock and river chemistry[27,29]. Once particles enter the surface ocean, a fraction of the ^{9}Be they carry is available for partial redissolution. If particles and the ^{9}Be they adsorbed are buried in marine sediment, some of the ^{9}Be is recycled back into deep water during early diagenesis.

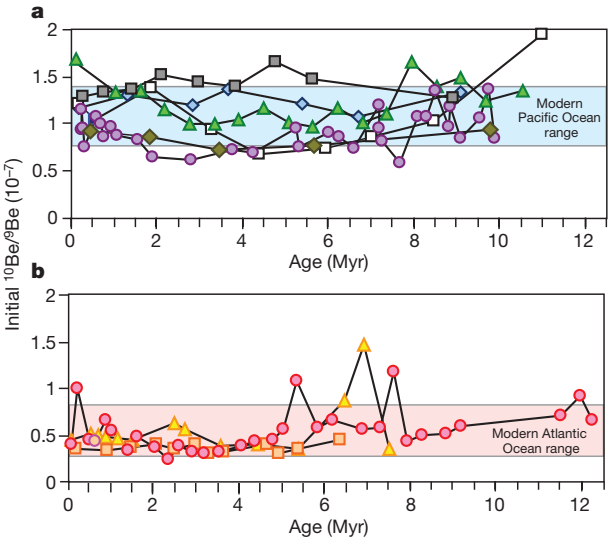

Figure 3 | Palaeo-ocean dissolved ^{10}Be/^{9}Be ratios as weathering proxies. Data from Pacific Ocean marine cores (RC12-65, violet circles) and hydrogenous ferromanganese crusts (F7-86-HW/CD29-2, blue diamonds; F10-89-CP/D11-1, white squares; VA13-2/KD237, green triangles; Nova IX/D137-01, grey squares; F10-89-CP/D27-2-1, brown/green diamonds) (**a**) and from the Atlantic Ocean hydrogenous ferromanganese crusts (ALV-539, yellow triangles; BM-1969.05, orange squares) and the Arctic Ocean marine core (ACEX, pink circles) (**b**). See Supplementary Information for data and references. Most individual measurements have a maximum 2-σ analytical error of ~10%, with lower uncertainty for recent measurements. Several outlier measurements within the data set have greater uncertainties. Because ^{10}Be decays with a half-life of 1.39 Myr, the original ^{10}Be/^{9}Be ratio at the time of deposition was calculated by assuming constant crust growth rates or sediment accumulation rates and correcting for decayed ^{10}Be for each sample interval[14]. An apparent circularity in this approach can be discounted because ^{10}Be-derived Pacific Fe–Mn crust growth rates agree with crust growth rates from Os isotope stratigraphy; decay-corrected Pacific Fe–Mn crust ^{10}Be/^{9}Be ratios agree with the corrected deep-sea core RC12-65 ^{10}Be/^{9}Be ratios, where magnetostratigraphy yields an independent age estimate; and ratios agree with each other within an ocean basin and also with young Fe–Mn surfaces within these basins[28]. These high-fidelity records of dissolved ^{9}Be and meteoric cosmogenic ^{10}Be in the open oceans imply ratios that fluctuate about a mean of 1×10^{-7} for Pacific sites and 0.5×10^{-7} for Atlantic and Arctic sites[28] (shown as horizontal bands shaded blue in **a** and pink in **b**). A fourfold increase in the recent flux of ^{9}Be-bearing terrigenous material (Fig. 1) would cause a decreasing trend in the ratio towards recent time, which is not observed in the three ocean basins sampled through time here. See Supplementary Information for additional details.

In each ocean basin, continental ^{9}Be is transferred from its fluvial point source by circulating ocean surface gyres that also carry ^{10}Be. These gyres rapidly homogenize the ^{10}Be and ^{9}Be to a characteristic isotope ratio on an ocean basin scale[30]. Importantly, scavenging of the element by particles affects both isotopes equally[30], such that variations in productivity or removal efficiency do not change the ^{10}Be/^{9}Be ratio, which represents only the differences in the delivery of terrigenous ^{9}Be to the deep ocean. Consequently, the ^{10}Be/^{9}Be ratio is lower in both the Atlantic and Arctic ocean basins than in the Pacific Ocean, owing to the larger ratio of coast length and ^{9}Be input to ocean area in the Atlantic, but both ratios were relatively

stable throughout the past 12 Myr (Fig. 3a, b). This stability demonstrates that the delivery of ^{9}Be derived from silicate weathering remained constant over this period when averaged over the million-year sampling interval of the Fe–Mn crusts.

We have provided evidence that on a global scale the chemical weathering flux was essentially constant over the past 10 Myr, and have found a mechanism that supports our questioning of observations of large increases in global physical erosion over the same interval. Therefore, we suggest that neither global erosion nor chemical weathering have been increased in any straightforward manner by climate change over the long (million-year) averaging timescale of our analysis, and that any simultaneous pulses in mountain building did not change the erosion or weathering flux globally. Hence, pulses in mountain uplift over this period might have been neither a direct cause nor an inevitable consequence of climate change[4].

Received 7 August 2009; accepted 22 March 2010.

1. Berner, R. A., Lasaga, A. C. & Garrels, R. M. The carbonate-silicate geochemical cycle and its effect on atmospheric carbon dioxide over the last 100 million years. *Am. J. Sci.* **205,** 641–683 (1983).
2. Raymo, M. E. & Ruddiman, W. F. Tectonic forcing of late Cenozoic climate. *Nature* **359,** 117–122 (1992).
3. Derry, L. A. & France-Lanord, C. Neogene growth of the sedimentary organic carbon reservoir. *Paleoceanography* **11,** 267–275 (1996).
4. Molnar, P. & England, P. Late Cenozoic uplift of mountain ranges and global climate change: chicken or egg? *Nature* **346,** 29–34 (1990).
5. Hay, W. W., Sloan, J. L. I. & Wold, C. N. The mass/age distribution of sediments on the ocean floor and the global rate of loss of sediment. *J. Geophys. Res.* **93,** 14933–14940 (1988).
6. Zhang, P., Molnar, P. & Downs, W. R. Increased sedimentation rates and grain sizes 2–4 Myr ago due to the influence of climate change on erosion rates. *Nature* **410,** 891–897 (2001).
7. Molnar, P. Late Cenozoic increase in accumulation rates of terrestrial sediment: how might climate change have affected erosion rates? *Annu. Rev. Earth Planet. Sci.* **32,** 67–89 (2004).
8. Riebe, C. S., Kirchner, J. W. & Finkel, R. C. Erosional and climatic effects in long-term chemical weathering rates in granitic landscapes spanning diverse climate regimes. *Earth Planet. Sci. Lett.* **224,** 547–562 (2004).
9. West, A. J., Galy, A. & Bickle, M. Tectonic and climatic controls on silicate weathering. *Earth Planet. Sci. Lett.* **235,** 211–228 (2005).
10. Wilkinson, B. H., McElroy, B. J., Kesler, S. E., Peters, S. E. & Rothman, E. D. Global geologic maps are tectonic speedometers – rates of rock cycling from area-age frequencies. *Geol. Soc. Am. Bull.* **121,** 760–779 (2009).
11. Royer, D. L., Berner, R. A., Montañez, I. P., Tabor, N. J. & Beerling, D. J. CO_2 as a primary driver of Phanerozoic climate change. *GSA Today* **14,** 4–10 (2004).
12. Pagani, M. & Liu, Z. LaRiviere, J. & Ravelo, A. C. High Earth-system climate sensitivity determined from Pliocene carbon dioxide concentrations. *Nature Geosci.* **3,** 27–30 (2010).
13. Sadler, P. M. The influence of hiatuses on sediment accumulation rates. *GeoRes. Forum* **5,** 15–40 (1999).
14. von Blanckenburg, F. & O'Nions, R. K. Response of beryllium and radiogenic isotope ratios in Northern Atlantic Deep Water to the onset of northern hemisphere glaciation. *Earth Planet. Sci. Lett.* **167,** 175–182 (1999).
15. Pagani, M., Caldeira, K., Berner, R. & Beerling, D. The role of terrestrial plants in limiting CO_2 decline for 24 million years. *Nature* **460,** 85–88 (2009).
16. Gabet, E. J. & Mudd, S. M. A theoretical model coupling chemical weathering rates with denudation rates. *Geology* **37,** 151–154 (2009).
17. Galy, V. *et al.* Efficient organic carbon burial in the Bengal fan sustained by the Himalayan erosional system. *Nature* **405,** 407–410 (2007).
18. Gilluly, J. Distribution of mountain building in geologic time. *Geol. Soc. Am. Bull.* **60,** 561–590 (1949).
19. Kuhlemann, J., Frisch, W., Székely, B., Dunkl, I. & Kázmér, M. Post-collisional sediment budget history of the Alps: tectonic versus climatic control. *Int. J. Earth Sci.* **91,** 818–837 (2002).
20. Métivier, F. Gaudemer, Y. Tapponier, P. & Klein, M. Mass accumulation rates in Asia during the Cenozoic. *Geophys. J. Int.* **137,** 280–318 (1999).
21. Ronov, A. B. Phanerozoic transgressions and regressions on the continents: a quantitative approach based on areas flooded by the sea and areas of marine and continental deposition. *Am. J. Sci.* **294,** 802–860 (1994).
22. Wilkinson, B. H. & McElroy, B. J. The impact of humans on continental erosion and sedimentation. *Geol. Soc. Am. Bull.* **119,** 140–156 (2007).
23. Wittmann, H., von Blanckenburg, F., Kruesmann, T., Norton, K. P. & Kubik, P. W. The relation between rock uplift and denudation from cosmogenic nuclides in river sediment in the Central Alps of Switzerland. *J. Geophys. Res.* **112,** F04010 (2007).
24. Kleman, J. & Hattestrand, C. Frozen-bed Fennoscandian and Laurentide ice sheets during the Last Glacial Maximum. *Nature* **402,** 62–64 (1999).
25. Marshall, S. J. & Clark, P. U. Basal temperature evolution of North American ice sheets and implications for the 100-kyr cycle. *Geophys. Res. Lett.* **29,** 2214–2218 (2002).
26. Roy, M., Clark, P. U., Raisbeck, G. M. & Yiou, F. Geochemical constraints on the regolith hypothesis for the middle Pleistocene transition. *Earth Planet. Sci. Lett.* **227,** 281–296 (2004).
27. Brown, E. T. *et al.* Continental inputs of beryllium to the oceans. *Earth Planet. Sci. Lett.* **114,** 101–111 (1992).
28. von Blanckenburg, F., O'Nions, R. K., Belshaw, N. S., Gibb, A. & Hein, J. R. Global distribution of beryllium isotopes in deep ocean water as derived from Fe-Mn crusts. *Earth Planet. Sci. Lett.* **141,** 213–226 (1996).
29. Frank, M. *et al.* The beryllium isotope composition of the Arctic Ocean. *Geochim. Cosmochim. Acta* **73,** 6114–6133 (2009).
30. Igel, H. & von Blanckenburg, F. Lateral mixing and advection of reactive isotope tracers in ocean basins: numerical modeling. *Geochem. Geophys. Geosys.* **1,** 1–19 (1999).

Supplementary Information is linked to the online version of the paper at www.nature.com/nature.

Acknowledgements J.K.W. gratefully acknowledges an Alexander von Humboldt Postdoctoral Fellowship.

Author Contributions J.K.W. and F.v.B. contributed equally to every aspect of the study.

Author Information Reprints and permissions information is available at www.nature.com/reprints. The authors declare no competing financial interests. Readers are welcome to comment on the online version of this article at www.nature.com/nature. J.K.W. is at the Department of Earth & Environmental Sciences, University of Pennsylvania, from July 2010. Correspondence and requests for materials should be addressed to F.v.B. (fvb@gfz-potsdam.de) or J.K.W. (jane.willenbring@sas.upenn.edu).